ARTICLE IN PRESS

WAMOT-01578; No of Pages 10

Wave Motion xxx (2011) xxx–xxx

Contents lists available at ScienceDirect

Wave Motion

journal homepage: www.elsevier.com/locate/wavemoti

Waves in microstructured solids and the Boussinesq paradigm

Jüri Engelbrecht [a,b], Andrus Salupere [a,*], Kert Tamm [a]

[a] Centre for Nonlinear Studies, Institute of Cybernetics at Tallinn University of Technology, Akadeemia tee 21, 12618, Tallinn, Estonia
[b] Estonian Academy of Sciences, Kohtu 6, 10130, Tallinn, Estonia

ARTICLE INFO

Article history:
Received 27 February 2011
Received in revised form 29 March 2011
Accepted 1 April 2011
Available online xxxx

Keywords:
Boussinesq paradigm
Microstructured solids
Solitons

ABSTRACT

The emergence of soliton trains and interaction of solitons are analyzed by using a Boussinesq-type equation which describes the propagation of bi-directional deformation waves in microstructured solids. The governing equation in the one-dimensional setting is based on the Mindlin model. This model includes scale parameters which show explicitly the influence of the microstructure in wave motion. As a result the governing equation has a hierarchical structure. The analysis is based on numerical simulation using the pseudospectral method. It is shown how the number of solitons in emerging trains depends on the initial excitation. The head-on collision of emerged solitons is not fully elastic due to radiation but the solitons preserve their identity after collision and the speed of solitons is retained while the radiation keeps a certain mean value. That is why we have kept through this paper the notion of solitons.

1. Introduction

The Boussinesq approximation for water waves, known from 1872, has served as a valuable basic model and a source for many extensions in order to include more physical effects. For example, the extensions take nonlinear effects as well as frequency dispersion into account and the extended models are able to describe layered fluid and internal waves. But the applications are not limited to water waves only. The general character of the Boussinesq and Boussinesq-type equations has been intensively studied because the equations of such a type occur also in dynamics of solids (waves in crystals, in rods, in microstructured materials, etc.), in theory of electric waves and so on. Christov, Maugin and Velarde [1–3] introduced the Boussinesq paradigm in order to grasp the following effects: (i) bi-directionality of waves; (ii) nonlinearity (of any order); (iii) dispersion (of any order, modeled by space and time derivatives of the fourth order at least). Christov et al. [4] have summarized the recent studies on properties of Boussinesq equation and its generalization for nonlinear waves.

Another important milestone for water waves was passed in 1895 when Korteweg and de Vries derived the unidirectional equation for describing waves in shallow water. This equation which is now known by their name – Korteweg–de Vries (KdV) equation – takes quadratic nonlinearity and cubic dispersion into account. The KdV equation is nowadays an iconic equation because of its solitonic solutions. Its rich history and impact to other studies are reflected by Weissert [5] in an excellent overview. Contemporary science knows a plethora of the KdV-type equations which differ from the standard KdV equation by more complicated nonlinearities and dispersion effects taken into account [6–10]. Such effects can be traced back to the Boussinesq-type equations but there is an essential difference between these two models — this is directionality. The Boussinesq equation is bi-directional (i.e., involves two waves propagating to right and left) while the KdV-type equations are uni-directional (i.e., involve just one wave). The methods for deriving uni-directional or evolution equations from bi-directional equations (or more general equations) are well known [11–13]. And again it is not only water waves but also waves in solids for which evolution equations are used in modeling of wave propagation.

* Corresponding author.
E-mail addresses: je@ioc.ee (J. Engelbrecht), salupere@ioc.ee (A. Salupere), kert@cens.ioc.ee (K. Tamm).

0165-2125/$ – see front matter © 2011 Elsevier B.V. All rights reserved.
doi:10.1016/j.wavemoti.2011.04.001

Please cite this article as: J. Engelbrecht, et al., Waves in microstructured solids and the Boussinesq paradigm, Wave Motion (2011), doi:10.1016/j.wavemoti.2011.04.001

In this paper we focus on nonlinear waves in microstructured solids which demonstrate rich dispersive effects over different scales. The basic bi-directional model is of a Mindlin-type [14,15] which corresponds to the Boussinesq paradigm [1]. In Section 2, the basic model is briefly discussed and in Section 3, the method for numerical analysis described. Section 4 forms the main part of the paper where emergence of soliton trains modeled by the Boussinesq type equation is analyzed and the head-on collision problems of solitons are described. These results demonstrate clearly the more general character of this model compared with a uni-directional approach. Finally, in Section 5 some general conclusions are drawn.

2. Model equations

The general idea of Mindlin [14] was to separate macro- and microstructure in continua and to formulate conservation laws for both structures also separately. This idea is elaborated by Engelbrecht et al. [15–18] including the dispersion analysis. The influence of nonlinearity may lead to the formation of solitary waves [16,17]. The model is rather general — it is shown that it can be formulated in terms of pseudomomentum [19] and in terms of internal variables [20,21]. Here we follow the 1D setting and recall only the main steps of derivation of the governing equation for longitudinal waves. The free energy function W is given in the following form: $W=W_2+W_3$ where W_2 is simplest quadratic function in terms of macrodisplacement u and microdeformation φ

$$W_2 = \frac{A}{2}u_x^2 + \frac{B}{2}\varphi^2 + \frac{C}{2}\varphi_x^2 + D\varphi u_x \tag{1}$$

and W_3 includes nonlinearities on both the macro- and microlevel

$$W_3 = \frac{N}{6}u_x^3 + \frac{M}{6}\varphi_x^3. \tag{2}$$

Here A, B, C, D, N and M are constants and right subindices here and further denote differentiation as usual. The kinetic energy K is determined by

$$K = \frac{1}{2}\rho u_t^2 + \frac{1}{2}I\varphi_t^2, \tag{3}$$

where I is the microinertia related to a microelement. By making use of the Euler–Lagrange equations, the basic 1D model for longitudinal waves is derived

$$\rho u_{tt} - \left(\frac{\partial W}{\partial u_x}\right)_x = 0, \quad I\varphi_{tt} - \left(\frac{\partial W}{\partial \varphi_x}\right)_x + \frac{\partial W}{\partial \varphi} = 0. \tag{4}$$

By introducingσ as the macrostress, η as the microstress and τ as the interactive force,

$$\sigma = \frac{\partial W}{\partial u_x}, \quad \eta = \frac{\partial W}{\partial \varphi_x}, \quad \tau = \frac{\partial W}{\partial \varphi}, \tag{5}$$

we arrive at the system of equation

$$\rho u_{tt} = \sigma_x, \quad I\varphi_{tt} = \eta_x - \tau. \tag{6}$$

Now we introduce the dimensionless variables

$$X = \frac{x}{L_0}, \quad T = \frac{\sqrt{A}t}{\sqrt{\rho}L_0}, \quad U = \frac{u}{U_0}, \tag{7}$$

where U_0 and L_0 are certain constants (e.g. the amplitude and the wavelength of the initial excitation) and also geometric parameters

$$\delta = \frac{l_0^2}{L_0^2}, \quad \varepsilon = \frac{U_0}{L_0}, \tag{8}$$

where l_0 is the characteristic scale of microstructure. By using an asymptotic procedure (for details see Ref. [15]) we obtain the final governing equation in the following form

$$U_{TT} - bU_{XX} - \frac{\mu}{2}\left(U_X^2\right)_X = \delta\left(\beta U_{TT} - \gamma U_{XX} + \frac{\lambda\sqrt{\delta}}{2}U_{XX}^2\right)_{XX}, \tag{9}$$

where

$$b = 1 - \frac{D^2}{AB},\ \mu = \frac{NU_0}{AL_0},\ \beta = \frac{ID^2}{\rho l_0^2 B^2},\ \gamma = \frac{CD^2}{AB^2 l_0^2},\ \lambda = \frac{D^3 MU_0}{AB^3 l_0^3 L_0}, \tag{10}$$

are constants. The related equation for the deformation $V = U_X$ reads

$$V_{TT} - bV_{XX} - \frac{\mu}{2}\left(V^2\right)_{XX} = \delta\left(\beta V_{TT} - \gamma V_{XX} + \frac{\lambda\sqrt{\delta}}{2}(V_X)_X^2\right)_{XX}. \tag{11}$$

Both Eqs. (9) and (11) belong clearly to the family of Boussinesq-type equations which are extensively studied by Christov et al. [4]. They include the mixed fourth-order space-time derivative like the regularized long-wave Boussinesq equations originally derived in fluid dynamics [22] and later in solid mechanics for waves in rods [23]. In the context of microstructured solids, this mixed derivative describes the effect of the inertia of the microstructure. One should mention here that the Boussinesq-type equation derived from the lattice dynamics for a chain of atoms involves only the fourth-order space derivatives [24]. The existence of two types of higher order derivatives in Eqs. (9) and (11) displays also explicitly the hierarchical character of the waves in the sense of Whitham [25]. Indeed, in derivation of Eqs. (9) and (11) the scale parameter δ plays the crucial role. If δ is small (the wavelength is large) then the waves are governed by the properties of the macrostructure and the operator

$$\Psi_{macro} = V_{TT} - bV_{XX} - \frac{\mu}{2}\left(V^2\right)_{XX} \tag{12}$$

has the leading role. If however δ is large (the wavelength is small) then the influence of the microstructure is more essential and the operator

$$\Psi_{micro} = \delta\left(\beta V_{TT} - \gamma V_{XX} + \frac{\lambda\sqrt{\delta}}{2}(V_X)_X^2\right)_{XX} \tag{13}$$

has the leading role. One should also note that Eqs. (9) and (11) are derived by the asymptotic analysis and the exact fourth-order one-equation model which corresponds to the system (6) of two second order equations includes also more fourth-order derivatives (with respect to space, time, and mixed space-time), see Engelbrecht et al. [15]. The dispersion analysis of two models – exact and approximated – has shown a good correspondence in a certain domain of material parameters [18].

3. Statement of the problem and numerical methods

When the Boussinesq paradigm related problems are studied, besides the analytical methods different numerical techniques play often important role [2,26–29]. In the present paper we study formation of soliton trains from a localized initial pulse and succeeding interaction between solitons. For this purpose the hierarchical model Eq. (11) is integrated numerically under localized initial conditions

$$V(X,0) = V_0 sech^2 B_0(X - X_0). \tag{14}$$

We use values $V_0 = 1$ and $B_0 = 0.01, \ldots 0.1$ for the initial pulse amplitude and width in numerical experiments discussed below; X_0 is the initial phase shift and is taken equal to half of the length of the space period. For material parameters fixed values of $\delta = 0.09$, $b = 0.7188$, $\beta = 56.0$, $\gamma = 9.3867$, $\mu = 1.1394$, $\lambda = 1.1470$ and the initial phase speed $c = 0$ are used (cf., for example Ref. [30]). For numerical integration the discrete Fourier transform (DFT) based pseudospectral method (PSM) [31,32] is used and therefore periodic boundary conditions

$$V(X,T) = V(X + 2L\kappa\pi, T),\ \kappa = 1,2,\ldots \tag{15}$$

are applied. Parameter L defines the length of the period. When interactions of solitons are studied, then the value $L = 800$ is used, but when the formation of soliton trains is studied, then longer space periods are needed and therefore values up to $L = 5500$ are used.

In a nutshell, the idea of the PSM is to approximate space derivatives making use of the DFT

$$\frac{\partial^m V}{\partial X^m} = F^{-1}\left[(ik)^m F(V)\right], \tag{16}$$

where F and F^{-1} denote the DFT and the inverse DFT, respectively, $k = 0, \pm 1, \pm 2, \ldots$ and i is imaginary unit and then to use standard ODE solvers for integration with respect to the time. The regular PSM algorithm is derived for $u_t = \Phi(u, u_x, u_{2x}, \ldots, u_{mx})$

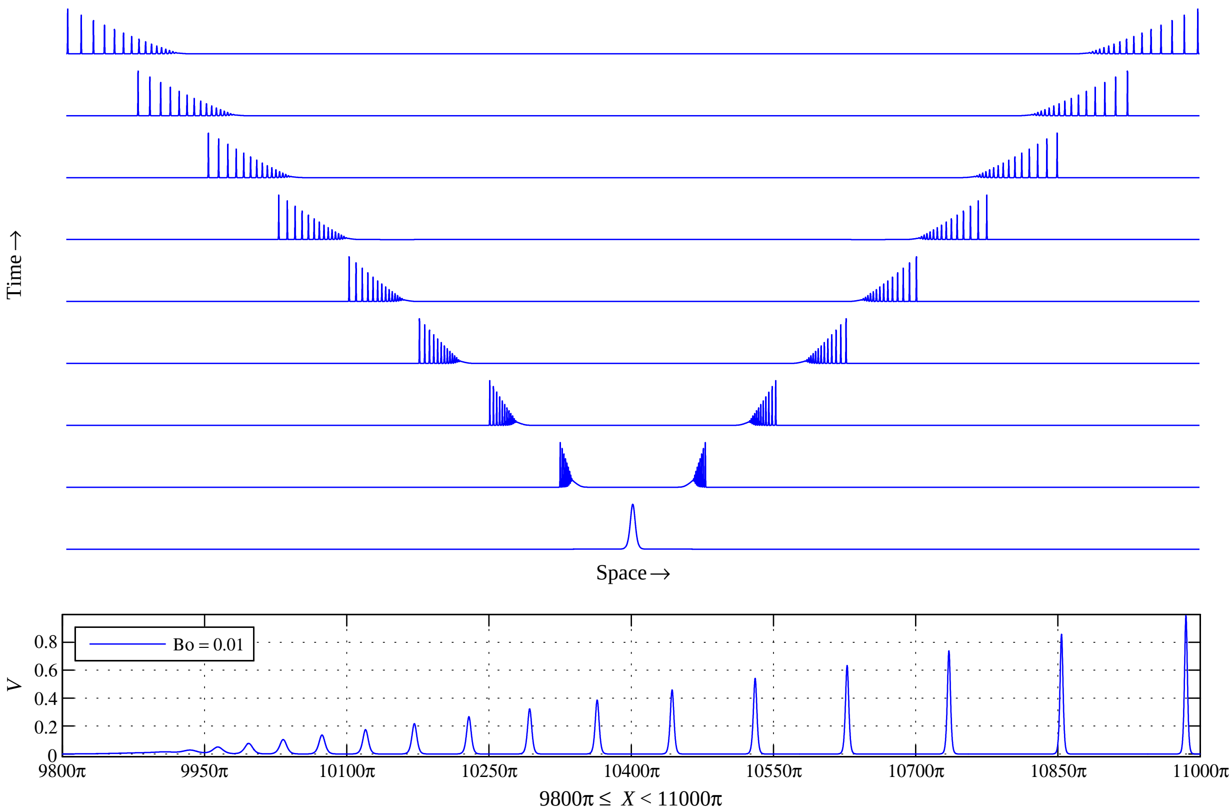

Fig. 1. Formation of trains of solitons for $B_0 = 0.01$. In upper panel single profiles are plotted at every $\Delta T = 2050$ and in lower panel — train of 16 solitons at $T = 16400$.

type equations. However, in our case we have a mixed partial derivative term $\delta\beta V_{TTXX}$ in Eq. (11) and therefore the standard PSM has to be modified [30,32,33]. First we introduce a new variable

$$\Phi = V - \delta\beta V_{XX} \tag{17}$$

and express variable V and its spatial derivatives in terms of variable Φ as follows:

$$V = F^{-1}\left[\frac{F(\Phi)}{1+\delta\beta k^2}\right], \quad \frac{\partial^m V}{\partial X^m} = F^{-1}\left[\frac{(ik)^m F(\Phi)}{1+\delta\beta k^2}\right]. \tag{18}$$

Now the hierarchical Eq. (11) is rewritten in form

$$\Phi_{TT} = \left(bV + \frac{\mu}{2}V^2 - \delta\gamma V_{XX} - \frac{\lambda\sqrt{\delta}}{2}\left[V_X^2\right]_X\right)_{XX}, \tag{19}$$

where variable V and its space derivatives are calculated in terms of the new variable Φ according to Eq. (18) and therefore after reducing it to a system of two first order differential equations the PSM can be applied.

4. Results and discussion

Eq. (11) is of the Boussinesq-type and therefore it can be predicted that two symmetric trains of solitons emerge from the initial bell shaped pulse in case of the initial phase speed $c = 0$. In Fig. 1 the formation of two soliton trains is presented for $B_0 = 0.01$ — the

Table 1
Number of solitons against the width of the initial pulse B_0.

B_0	0.01	0.02	0.03	0.04	0.05	0.06	0.07	0.08	0.09	0.1
N_S	16	9	6	5	4	3	2	2	2	2

Table 2
Soliton amplitudes V_i against the width of the initial pulse B_0.

i \ B_0	0.01	0.02	0.03	0.04	0.05	0.06	0.07	0.08	0.09	0.1
1	0.991	0.929	0.873	0.823	0.778	0.737	0.700	0.666	0.634	0.606
2	0.858	0.689	0.549	0.431	0.332	0.249	0.178	0.120	0.073	0.038
3	0.739	0.502	0.326	0.197	0.104	0.042				
4	0.634	0.355	0.175	0.063	0.011					
5	0.541	0.242	0.076	0.007						
6	0.459	0.154	0.019							
7	0.387	0.089								
8	0.323	0.041								
9	0.267	0.013								
10	0.217									
11	0.174									
12	0.136									
13	0.104									
14	0.076									
15	0.050									
16	0.028									

upper panel demonstrates the formation process ($\Delta T = 2050$ and last line at $T = 16400$) and the lower panel shows the train of 16 solitons at $T = 16400$. For initial pulses of different width, the soliton train consists of different number of solitons. In Table 1 the number of solitons N_S is presented against the width of the initial pulse B_0. It is clear, that the wider the initial pulse (the lower the value of B_0), the higher the number of emerged solitons.

In Table 2 amplitudes of emerged solitons V_i are presented against the width of the initial pulse B_0. The amplitudes are measured at the end of the formation period, i.e., just before the first interaction between the left- and the right-propagating soliton trains starts. After solitons are emerged they propagate indeed without any amplitude change as shown in Fig. 2 for $B_0 = 0.01$ up to $T = 16400$. In Table 3 speeds of the four highest solitons are presented against the width of the pulse B_0. It is clear that as usual, the higher the soliton the faster it is. In Fig. 3 speeds of four higher solitons are plotted against their amplitudes for

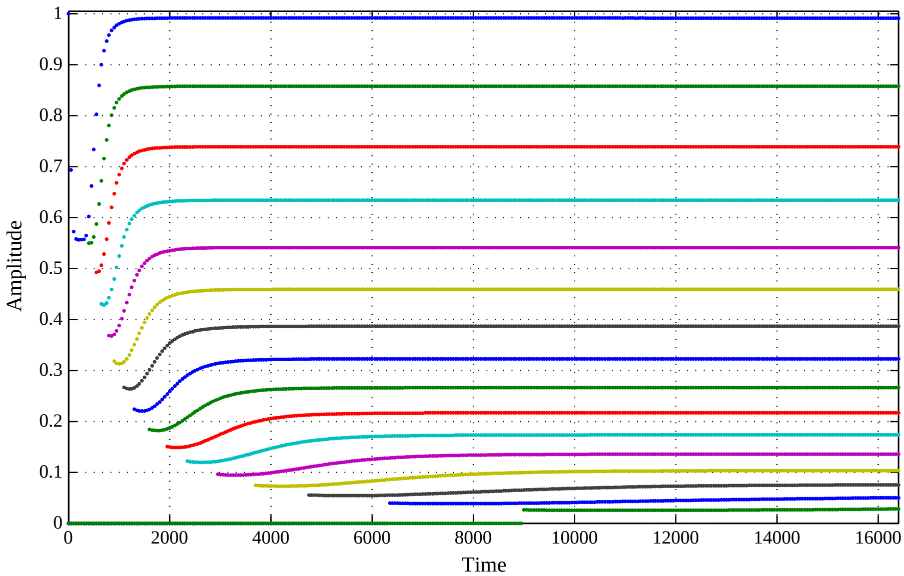

Fig. 2. Emergence of soliton trains: amplitudes of solitons against time for $B_0 = 0.01$; $0 \leq T \leq 16400$.

Table 3
The speed of the four highest solitons against the width of the initial pulse B_0.

i \ B_0	0.01	0.02	0.03	0.04	0.05	0.06	0.07	0.08	0.09	0.1
1	1.0467	1.0353	1.0249	1.0156	1.0071	0.9994	0.9923	0.9857	0.9797	0.9740
2	1.0222	0.9902	0.9630	0.9395	0.9193	0.9018	0.8868	0.8741	0.8635	0.8549
3	0.9998	0.9536	0.9181	0.8909	0.8711	0.8568				
4	0.9798	0.9241	0.8868	0.8619						

Please cite this article as: J. Engelbrecht, et al., Waves in microstructured solids and the Boussinesq paradigm, Wave Motion (2011), doi:10.1016/j.wavemoti.2011.04.001

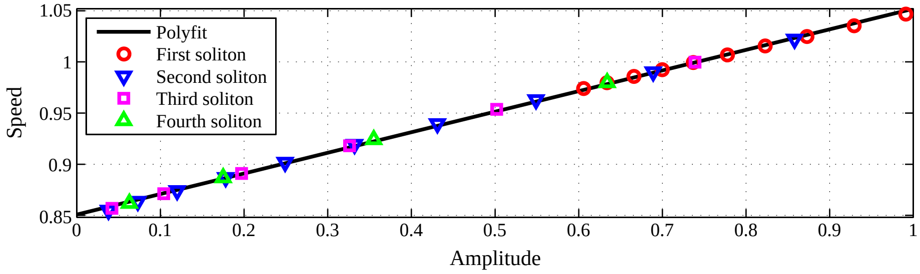

Fig. 3. Soliton speed against amplitude.

$0.01 \le B_0 \le 0.1$ (speeds and amplitudes are calculated before the interactions between soliton trains start). It is clear that soliton speed is linearly dependent on their amplitudes. Straight solid line $c_s = 0.2013V_s + 0.8507$ fits the data-set by means of least squares (V_s is the amplitude of the soliton and c_s is its speed). From Eq. (11) (or Eq. (9)) it follows that the characteristic speed $c_0 = \sqrt{b}$ and in the present case $c_0 = 0.8478$. Consequently, if the amplitude of the soliton approaches zero the speed of the soliton approaches the characteristic speed, i.e., $lim_{V_s \to 0 c_s \approx c_0}$. The difference is caused by the fact that the straight line is generated by using the least squares fit. It should be noted that in one-wave equations (for example the KdV equation) usually the moving frame of reference is used. The speed c_0 would be the speed of the moving frame of reference in such a case. However, as Eq. (11) is a two-wave equation, in the present case it makes sense to stay in the fixed frame of reference.

In all considered cases solitons propagate to the right and left at the same speed and therefore the solutions are symmetric with respect to the initial phase shift X_0.

The time-slice plot in Fig. 4 characterizes the emergence of two soliton trains and succeeding interactions between solitons for $B_0 = 0.03$. Due to the periodic boundary conditions the behavior of emerged trains can be traced throughout four interactions (for

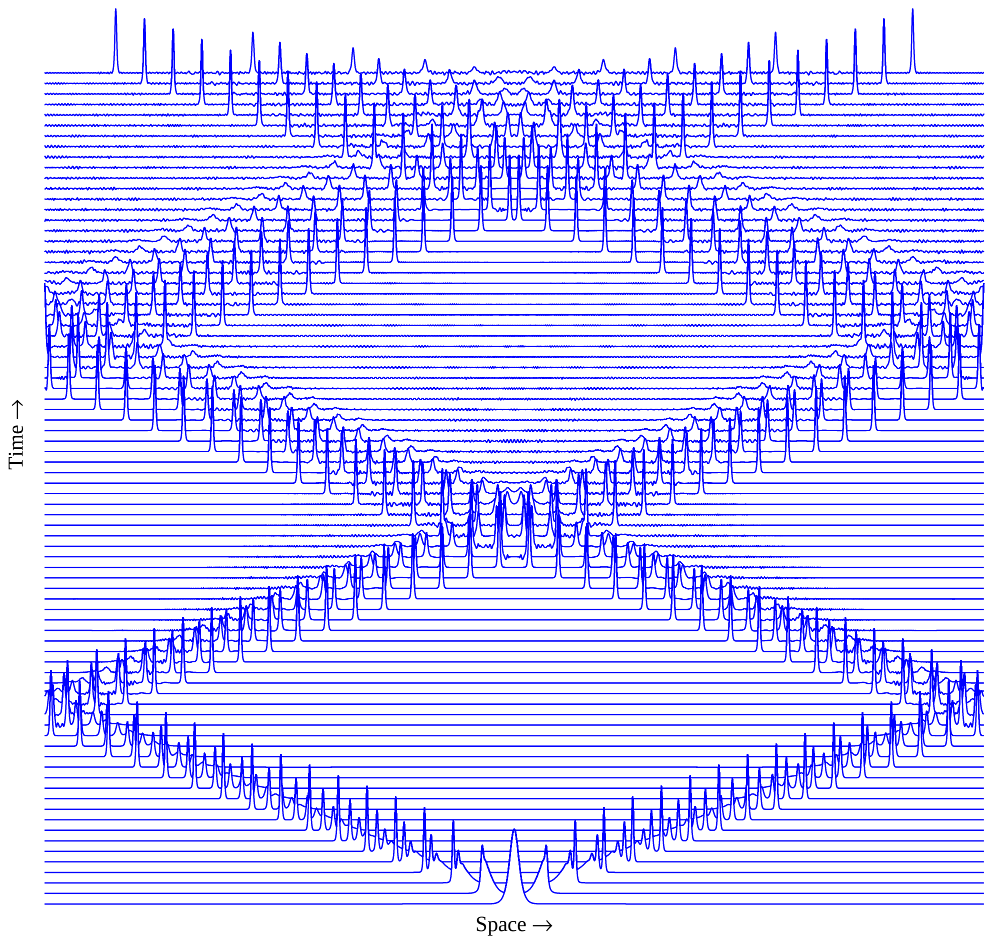

Fig. 4. Formation of soliton trains and interaction of solitons (waveprofiles are plotted at every $\Delta T = 150$) for $B_0 = 0.03$; $0 \le T \le 12000$.

single solitons the number of interactions is $4 \times 5 = 20$) for $0 \leq T \leq 12000$. In order to compare the solutions that correspond to different values of the pulse width B_0 single waveprofiles for $B_0 = 0.01 \ldots 0.1$ are plotted at $T = 2280$ and $T = 7000$ in Figs. 5 and 6, respectively. Trains, presented in these Figures propagate to the right. Trains in Fig. 5 can be called initial trains, because they are plotted before the first interactions. Trains in Fig. 6 are plotted after the second interactions (just before the third interactions will start). At time moment $T = 7000$ all solitons which can be detected in Fig. 6 have passed two interactions with all solitons from the train propagating to the left. The x–V space-scale is the same for all plots in Figs. 5 and 6. Therefore one can estimate the different speeds and amplitudes of single solitons for different values of parameter B_0 (the width of the pulse). Initial soliton trains in Figs. 1 and 5 are different, because of the different length of space periods. When the emergence of trains is studied, the space periods of different length are used for different values of the parameter B_0 — the length for $B_0 = 0.01$ is 11000π. When the interaction is studied, the length of the space period equals to 1600π for all values of B_0. For wider initial pulses ($0.01 \leq B_0 \leq 0.06$) the initial pulse is morphed into a train of solitons without a distinguishable tail (see Figs. 1, 4 and 5). However, if the initial pulse is so narrow that only a train of two solitons emerges ($0.07 \leq B_0 \leq 0.1$), then besides the solitons a distinguishable oscillating tail emerges (see Fig. 5).

In order to verify the usage of the term soliton, one must analyze the character of interactions. By definition a solitary wave can be called soliton if it interacts with other such entities elastically, i.e., if it restores after interaction its speed and amplitude. In the case of soliton emergence, the spatial period of initial pulses has been taken long enough, so in practice this part of the study is non-periodic even if the applied numerical method requires periodic boundary conditions. In the case of interactions, however, the results can be interpreted as a non-periodic setup with K identical initial conditions and correspondingly longer initial spatial period, where the K is the number of interactions.

Time-slice plot in Fig. 4 demonstrates that really all emerged solitons conserve their identity throughout interactions. However, it is obvious that each interaction produces a certain radiation which first of all influences the shape of the lower-amplitude solitary waves. Of course, observing the time-slice plot is not sufficient in order to verify the solitonic behavior of emerged solitary waves. Analysis of trajectories of solitary waves demonstrates that between interactions they propagate at constant speed. In Fig. 7 amplitudes of four higher solitons (waveprofile maxima) are plotted against time over the whole integration interval, i.e., for $0 \leq T \leq 31000$. In order to focus on the behavior of solitons between interactions, the maxima which correspond to interactions are abandoned in this figure. It is clear, that one can speak about constant amplitudes of solitons before the first interactions only (the

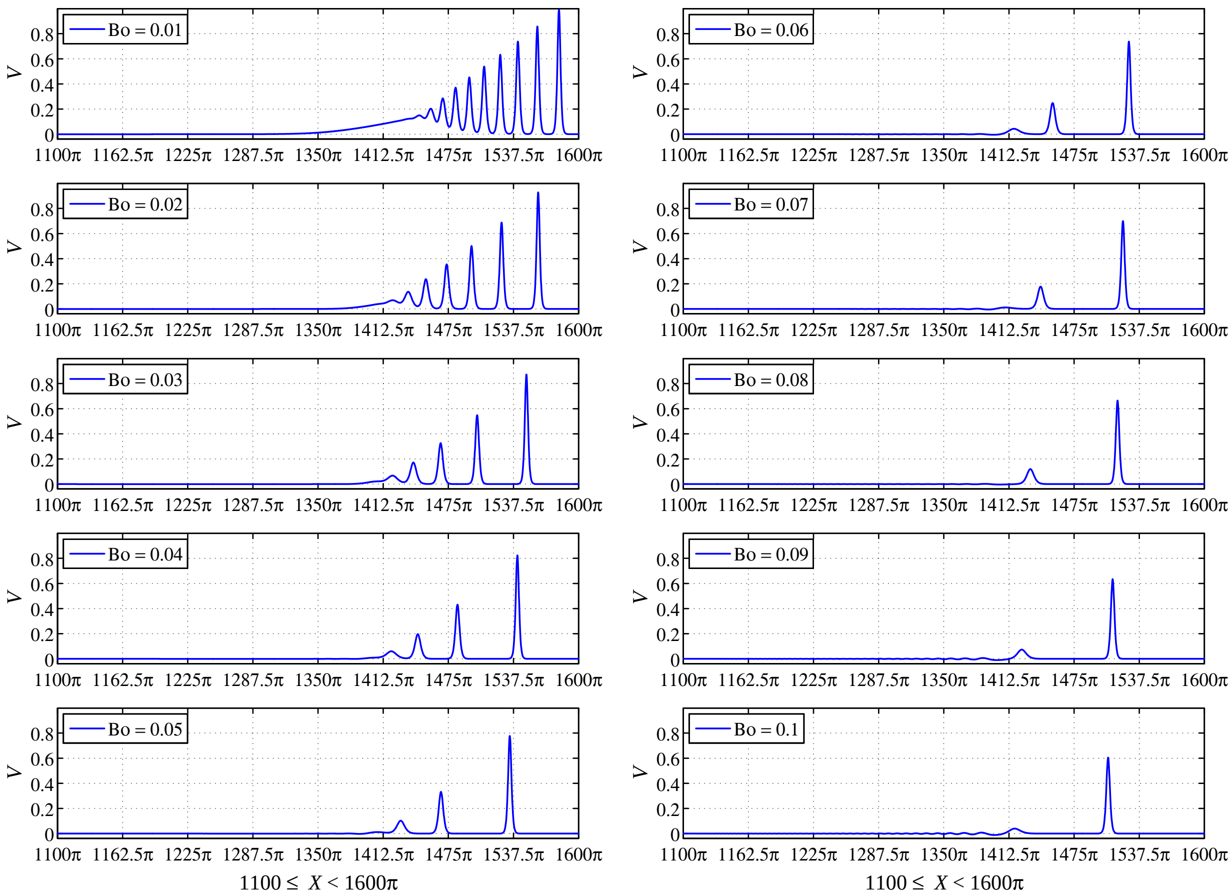

Fig. 5. Single waveprofiles at $T = 2280$ for $B_0 = 0.01 \ldots 0.1$.

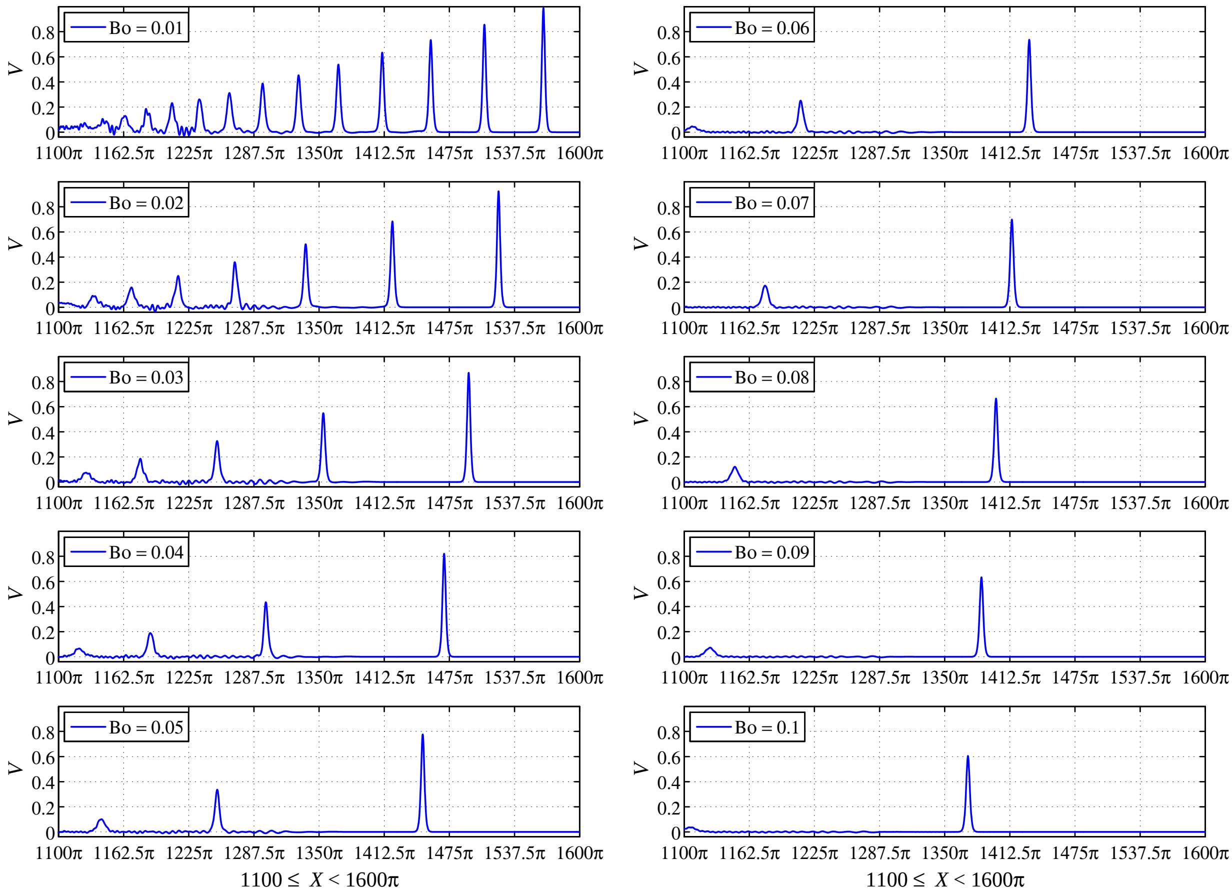

Fig. 6. Single waveprofiles at $T = 7000$ for $B_0 = 0.01 \ldots 0.1$.

highest soliton has constant amplitude also between the first and the second and the second and the third interactions between the two soliton trains). The amplitudes of the lower solitons start to oscillate just after the first interaction. This is due to the radiation, generated during interactions. However, these oscillations take place about a certain mean level. For the first soliton this

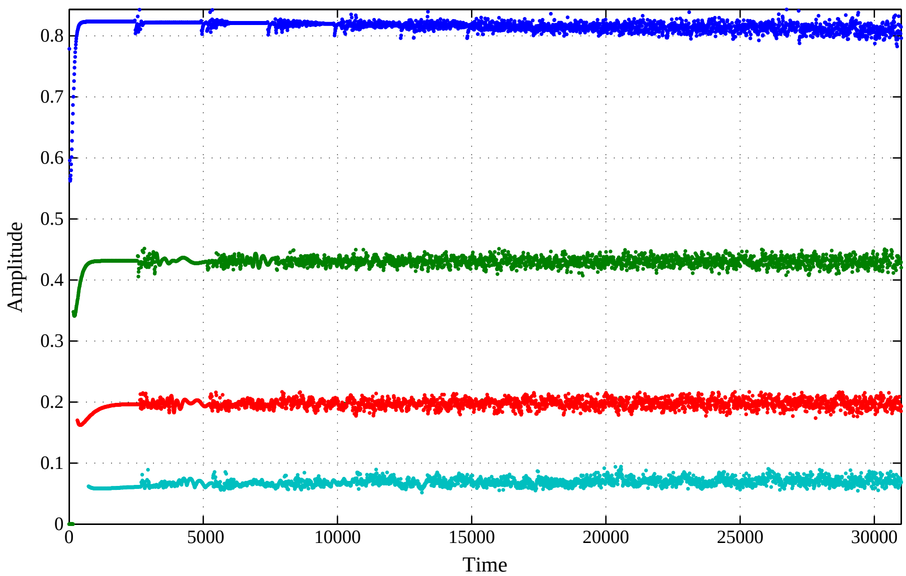

Fig. 7. Interactions of soliton trains: amplitudes of solitons against time for $B_0 = 0.04$; $0 \le T \le 31000$.

mean level decreases and for the fourth soliton increases slightly. This means that the interactions are not completely elastic and a certain exchange of energy takes place between different solitons and solitons and the radiation (radiating structure).

5. Conclusions and final remarks

The Boussinesq-type bi-directional models (9) and (11) involve fourth order derivatives which characterize the influence of dispersion. It is evident how inertial and elastic properties of the microstructure are inscribed into various terms in the governing equation. Compared with the uni-directional KdV-type model, the present one is without any doubt closer to reality. Indeed, such a bi-directional model, called also a double-dispersion model is used to describe nonlinear deformation waves in rods [34,35]. For model (11) it has been shown that the resulting uni-directional KdV-type equation involves the usual third order dispersive term with a coefficient which combines both inertial and elastic properties [36].

The present approach demonstrates clearly the most interesting feature for nonlinear waves in dispersive medium — the emerging of soliton trains. The emerging solitons display all the characteristics of classical solitons. This model permits also to study the head-on collision of solitons. The study reveals that the interaction is not fully elastic. The numerical method used for the analysis is of high accuracy and tested for many complicated cases [32], so the demonstrated radiation must have physical reasons. The additional oscillations of soliton amplitudes after head-on collision, however, are more distinguishable for solitons with lower amplitudes but these oscillations take place about a certain mean level. As far as the identity of solitons is preserved after interactions, we kept throughout the paper the notion of solitons, although strictly speaking, we should use the term 'quasi-solitons'. The process of emerging and propagating such quasi-solitons needs more studies in order to understand the process in non-integrable systems and also to agree on terminology. Quasi-solitons are characteristic to the real world and they do not interact completely elastically like "pure solitons" which are characteristic for highly idealized systems. It is clear that the interaction process of such quasi-solitons needs also more detailed analysis like it is done for the KdV-solitons [37] and for 'clean' solitary waves following [38]. The results of the present paper together with results of paper [39] can be applied for elaborating and enhancing of nondestructive testing algorithms.

Acknowledgments

The research was supported by the Estonian Science Foundation grant no. 7035. The authors would like to thank reviewers for very useful remarks.

References

[1] G.A. Maugin, C.I. Christov, Nonlinear duality between elastic waves and quasi-particles, in: C.I. Christov, A. Guran (Eds.), Selected Topics in Nonlinear Wave Mechanics, Birkhäuser, Boston, 2002, pp. 117–160.
[2] C. Christov, M. Velarde, Inelastic interaction of Boussinesq solitons, Int. J. Bifur. Chaos 4 (1994) 1095–1112.
[3] C. Christov, G. Maugin, M. Velarde, Well-posed Boussinesq paradigm with purely spatial higher-order derivatives, Phys. Rev. E 54 (1996) 3621–3638.
[4] C. Christov, G. Maugin, A. Porubov, On Boussinesq's paradigm in nonlinear wave propagation, C. R. Mécanique 335 (2007) 521–535.
[5] T.P. Weissert, The genesis of simulation in dynamics, Pursuing the Fermi–Pasta–Ulam problem, Springer, New York, 1997.
[6] T.B. Benjamin, J.L. Bona, J.J. Mahony, Model equations for long waves in nonlinear dispersive systems, Philos. Trans. R. Soc. Lond. Ser. A 272 (1972) 47–78.
[7] O. Ilison, A. Salupere, On the propagation of solitary pulses in microstructured materials, Chaos Solitons Fractals 29 (2006) 202–214.
[8] C. Christov, M. Velarde, Dissipative solitons, Phys. D 86 (1995) 323–347.
[9] A. Salupere, L. Ilison, J. Engelbrecht, O. Ilison, On solitons in microstructured solids and granular materials, Math. Comput. Simul. 69 (2005) 502–513.
[10] A. Porubov, G. Maugin, V. Gursky, V. Krzhizhanovskaya, On some localized waves described by the extended KdV equation, C. R. Mécanique 333 (2005) 528–533.
[11] T. Taniuti, K. Nishihara, Nonlinear Waves, Pitman, London, 1983 (in Japanese 1977).
[12] A. Jeffrey, T. Kawahara, Asymptotic Methods in Nonlinear Wave Theory, Pitman, Boston, 1982.
[13] J. Engelbrecht, Nonlinear Wave Processes of Deformation in Solids, Pitman, London, 1983.
[14] R.D. Mindlin, Micro-structure in linear elasticity, Arch. Rat. Mech. Anal. 16 (1964) 51–78.
[15] J. Engelbrecht, A. Berezovski, F. Pastrone, M. Braun, Waves in microstructured materials and dispersion, Phil. Mag. 85 (2005) 4127–4141.
[16] J. Janno, J. Engelbrecht, Solitary waves in nonlinear microstructured materials, J. Phys. A: Math. Gen. 38 (2005) 5159–5172.
[17] J. Engelbrecht, A. Berezovski, A. Salupere, Nonlinear deformation waves in solids and dispersion, Wave Motion 44 (2007) 493–500.
[18] T. Peets, M. Randrüüt, J. Engelbrecht, On modelling dispersion in microstructured solids, Wave Motion 45 (2008) 471–480.
[19] G.A. Maugin, Material Inhomogeneities in Elasticity, Chapman & Hall, London, 1993.
[20] P. Ván, A. Berezovski, J. Engelbrecht, Internal variables and dynamic degrees of freedom, J. Non-Equilib. Thermodyn. 33 (2008) 235–254.
[21] A. Berezovski, J. Engelbrecht, G.A. Maugin, Generalized thermomechanics with dual internal variables, Arch. Appl. Mech. 81 (2011) 229–240.
[22] P. Bois, Joseph Boussinesq (1842–1929): a pioneer of mechanical modelling at the end of the 19th Century, C. R. Mécanique 335 (2007) 479–495.
[23] L.A. Ostrovskii, A.M. Sutin, Nonlinear elastic waves in rods, J. Appl. Math. Mech. (English translation PMM) 41 (1977) 543–549.
[24] G. Maugin, Nonlinear Waves in Elastic Crystals, Oxford Univ, Press, Oxford, 1999.
[25] G. Whitham, Linear and Nonlinear Waves, John Wiley & Sons, New York, 1974.
[26] C.I. Christov, G.A. Maugin, An implicit difference scheme for the long-time evolution of localized solutions of a generalized Boussinesq system, J. Comput. Phys. 116 (1995) 39–51.
[27] T. Marinov, C. Christov, R. Marinova, Novel numerical approach to solitary-wave solutions identification of Boussinesq and Korteweg–de Vries equations, Int. J. Bifur. Chaos 15 (2005) 557–565.
[28] C.I. Christov, An energy-consistent dispersive shallow-water model, Wave Motion 34 (2001) 161–174.
[29] M. Christou, C. Christov, Fourier–Galerkin method for 2D solitons of Boussinesq equation, Math. Comput. Simul. 74 (2007) 82–92.
[30] A. Salupere, K. Tamm, J. Engelbrecht, Numerical simulation of interaction of solitary deformation waves in microstructured solids, Int. J. Non-Linear Mech. 43 (2008) 201–208.
[31] B. Fornberg, A Practical Guide to Pseudospectral Methods, Cambridge University Press, Cambridge, 1998.
[32] A. Salupere, Pseudospectral method and discrete spectral analysis, in: E. Quak, T. Soomere (Eds.), Applied Wave Mathematics, Springer, 2009, pp. 301–334.
[33] K. Tamm, A. Salupere, On propagation of solitary waves in Mindlin-type microstructured solids, Proc. Estonian Acad. Sci. 59 (2010) 118–125.

[34] A.V. Porubov, Amplification of Nonlinear Strain Waves in Solids, World Scientific, Hong Kong, 2003.
[35] A. Samsonov, Strain Solitons in Solids and How to Construct Them, CRC Press, Boca Raton, 2001.
[36] M. Randrüüt, M. Braun, On one-dimensional solitary waves in microstructured solids, Wave Motion 47 (2010) 217–230.
[37] A. Salupere, J. Engelbrecht, P. Peterson, Long-time behaviour of soliton ensembles. Part I—emergence of ensembles, Chaos Solitons Fractals 14 (2002) 1413–1424.
[38] H. Kalisch, J. Bona, Models for internal waves in deep water, Discrete Contin. Dynam. Systems 6 (2000) 1–20.
[39] J. Janno, J. Engelbrecht, An inverse solitary wave problem related to microstructured materials, Inverse Problems 21 (2005) 2019–2034.